HAPTICS SYMPOSIUM '16, APRIL 8–11, 2016, PHILADELPHIA, PENNSYLVANIA, USA
978-1-5090-0903-9/16/$31.00 ©2016 IEEE

eShiver: Force Feedback on Fingertips through Oscillatory Motion of an Electroadhesive Surface

Joseph Mullenbach[1], Michael Peshkin[2], and J. Edward Colgate[3]

Abstract— **We introduce a new haptic force feedback device – the eShiver – for creating lateral shear force on the bare fingertip. The eShiver uses in-plane oscillatory motion of a variable-friction electroadhesive surface operating at 55Hz. A set of experiments performed with an artificial finger is used to elucidate the performance characteristics of this device. A maximum net lateral force of ±300mN is achieved, and net force is shown to be a function of velocity, applied voltage, and the phase between them. We propose a simple lumped parameter model for the system consisting of a lateral impedance and a voltage controlled "friction switch." We also discuss the limitations and areas of possible improvement for this method of force generation.**

I. INTRODUCTION

By relating forces and motions, haptic force feedback devices create bilateral interactions between the user and a virtual environment. Bilateral interaction is the key to simulating dynamic and mechanically complex virtual environments such as surgery [1] and product assembly [2]. For some years, our group has been interested in bringing bilateral interaction to touchscreens with the expectation that doing so will significantly extend the metaphor of direct manipulation [3], [4], [5]. In addition to interacting with objects in a planar dynamic environment, a laterally forcing device can also convey the perception of texture and of shape protruding from the plane [6], [7], [8]. Unlike conventional force feedback devices however, the touchscreen context does not readily allow forces to be applied through a handle or thimble. Instead, it is necessary to apply forces directly to the bare fingertips. Previous approaches have accomplished this strictly through the use of surface vibrations, but have limited force magnitude. In this paper, we introduce a new approach that combines lateral vibrations with electroadhesion as a step toward high force capability.

II. BACKGROUND

A. Lateral Forcing Surfaces

Past approaches to applying force feedback to fingertips can be grouped into two basic categories. The first category includes kinematic devices with a large range of motion relative to the finger size. This includes devices which slide a thimble-like finger holder or transparent overlay across a surface and control force with electric motors mounted past the edge of the surface [5], [8], [9]. These devices are capable of applying high forces to the finger, but require a relatively complex mechanical design and are physically large.

[1]Northwestern University mullenbach@u.northwestern.edu
[2]Northwestern University peshkin@northwestern.edu
[3]Northwestern University colgate@northwestern.edu

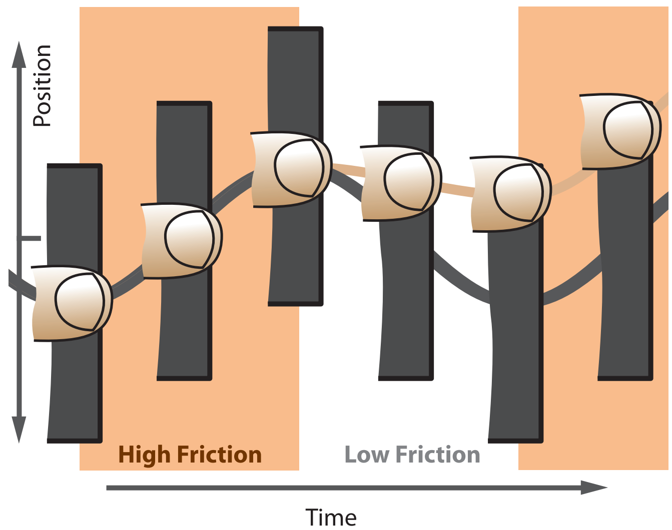

Fig. 1. Progression of actuation. As the surface slides forward, voltage is applied and the finger is stuck down to the moving surface creating a positive force. As the surface slides back, friction is reduced by controlling the voltage to zero, allowing the finger to slide across the moving surface.

The second category involves small motions relative to the finger size which oscillate and in which friction force is in some way varied to create a rectified net force in one direction. The LateralPaD used vibrations in the normal and lateral directions at $22kHz$ and with amplitudes up to $2\mu m$ [4]. Its operating principle was the same as a traveling wave ultrasonic motor in that its rectification of lateral force comes from variation in contact force due to the normal vibration. The LateralPad achieved net lateral forces of up to $\pm 50mN$.

B. ShiverPaD

Another approach within this category of oscillating friction force rectifiers was demonstrated by the ShiverPad [3]. As is shown in Figure 1, the operating principle is to use an actively controlled "friction switch" which can be turned on and off in phase as the surface oscillates laterally, or "shivers." As the plate moves forward, the friction switch is set high, fixing the skin against the plate and generating a high reaction force in the skin. As the plate moves in reverse, the friction switch is set low, allowing the skin to slip against the surface, generating only a small reaction force in the skin. Therefore, averaged across a single cycle, the net force on the skin is positive. This sequence is repeated every cycle to create a rectified DC force.

Specifically, the ShiverPad used an ultrasonic friction reducing surface, a "TPad," as the friction switch [10]. It was able to create lateral forces on the bare fingertip of up to $\pm 100mN$ at an actuation frequency of $854Hz$. This is near the edge of the tactile perceptual range, but within the audible range.

C. Johnsen Rahbek Electroadhesion

The eShiver uses the same basic operating principle as the ShiverPaD, while introducing the use of the Johnsen Rahbek type electroadhesion as the friction switch. The Johnsen Rahbek electroadhesion makes use of a high contact resistance and a low current to establish a large potential difference across the gap between two surfaces in close contact [11]. The voltage across the gap acts as an electrostatic actuator, pulling the surfaces into more intimate contact and increasing the friction force. While the ShiverPad was able to produce net forces up to $100mN$, forces several times larger would be desirable. Electroadhesion has the potential to increase the range and maximum magnitude of the friction force while reducing the complexity of the mechanical design as it is a “solid state” method of friction switching. Shultz et al. demonstrated that the Johnsen Rahbek effect could be used to increase the frictional force acting on a human fingertip by approximately $1-2N$ at relevant levels of normal force [12].

III. MODEL SYSTEM

The model explained in [3] and illustrated in Figure 1 gives a rough understanding of how the ShiverPaD and eShiver create a net force. However, as a conceptual model it does not predict the magnitude of that force. Moreover, it is unclear what physical effects fundamentally limit force magnitude and operating frequency. Seeking a more nuanced understanding of how this force is produced, we have begun developing a model to predict and optimize eShiver performance.

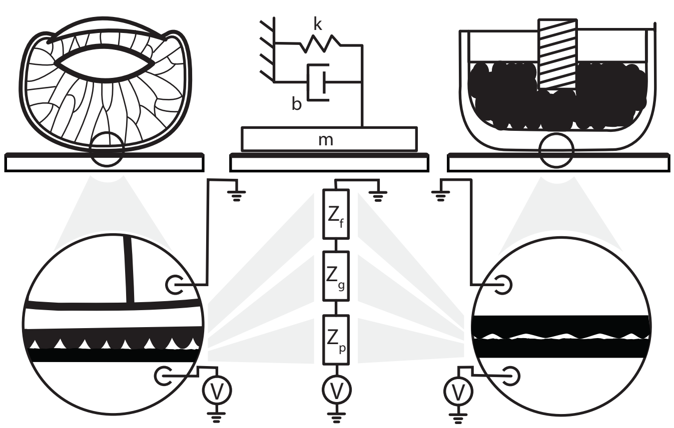

Fig. 2. Cutaway views and mechanical (top) and electrical (bottom) models of the human (left) and artificial (right) fingertips. The mechanical model is a spring and damper in parallel attached to a mass driven by a velocity source through a frictional interface. The electrical model is a voltage applied across three impedances in series representing the lumped equivalent impedance of the finger Z_f, the gap Z_g and the plate Z_P.

A. Lateral Force Generation

One key aspect of the model is the relationship between lateral motion and lateral force. In general, since our devices are much more massive than the fingertip, we will consider them to be high impedance lateral motion sources. With the actuation known, the lateral impedance of the fingertip is then needed to predict force. Biological material is commonly described with a viscoelastic Kelvin-Voigt model with an inertial element [14]. This model with the relevant mass (m), spring constant (k), and damping constant (b) is shown in Figure 2. Wiertlewski et al. conducted an extensive study which showed this model to be valid for shear impedance of the human fingertip in two contact configurations, and reported parameter values for seven subjects [13].

B. Friction Switch

Another key aspect of the model is the “strength” of the friction switch. To model the frictional interface, we define a frictional limit above which the fingertip slides, and maintains a constant force at that limit. This is equivalent to a Coulomb friction model in which the kinetic friction is equal to the static friction. As is described in [12] and elsewhere, the attractive force and (by assuming a constant coefficient of friction) lateral force due to electroadhesion are proportional to the square of the voltage across the gap $F \propto V_g^2$. While the voltage across the gap is the relevant voltage, it unfortunately cannot be controlled or measured directly. Instead, the total voltage is controlled and the electrical system must be modeled to estimate the gap voltage.

The simplified electrical model of this system as proposed in [12] is shown in Figure 2. The overall impedance, Z_t, is composed of three impedances in series- a bulk impedance of the finger, Z_f, a bulk impedance of the plate, Z_p, and a “gap” impedance, Z_g. While Z_f and Z_p are determined by the material properties and geometry in the usual way, Z_g is a function of the contact between them. At a microscopic level, the majority of the surface is not in “real” contact. Rather, asperity tips come into contact and a gap is created everywhere else. These asperities in contact create a resistive path for current to flow, while the gap effectively creates a capacitive surface pair on which charge can accumulate.

C. Generation of Net Force

As is shown in Figure 3 we define F_S as the actual shear force transmitted across the interface, while F_Y and F_Z represent the lateral and normal forces measured at the load cell. Additionally, we define three theoretical force limits. F_L is defined as the lateral force that would develop due the plate motion applied to the lateral fingertip impedance assuming the finger is stuck to the plate. F_{mn} is defined as the minimum friction force when the friction switch is off, and F_{mx} is defined as the maximum friction force when the friction switch is on, which is a function of the applied voltage V.

As the plate moves forward, a force F_S is transmitted in shear across the frictional interface, reacted by the finger.

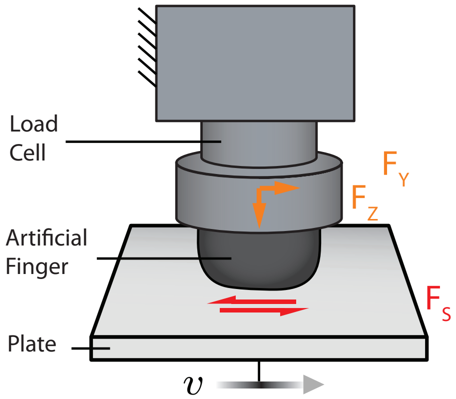

Fig. 3. Artificial finger and plate oscillating at velocity v. F_Y and F_Z are the lateral and normal forces measured at the force sensor. F_S is the shear force across the frictional interface.

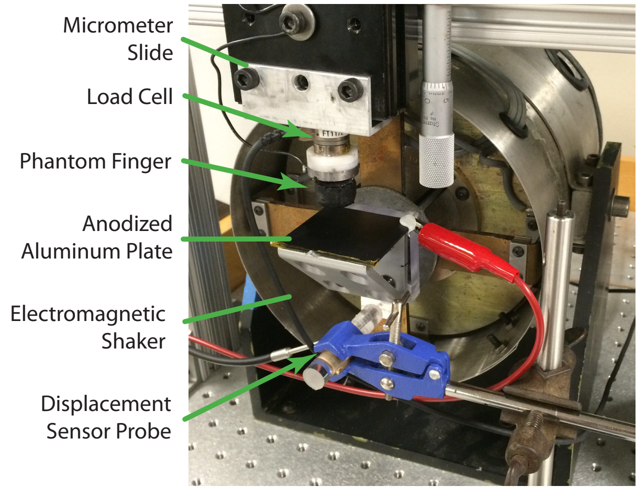

Fig. 4. eShiver Experimental Apparatus.

Initially the finger is stuck to the plate, and F_S is equal to F_L. This force increases up to the maximum friction force, F_{mx}, where the finger starts to slip. In the reverse direction the magnitude of F_S again increases, but this time only up to the minimum friction force F_{mn}.

$$-F_{mn} < F_S < F_{mx}$$

In addition to these friction force limits, F_S can never exceed the maximum force due to lateral impedance, F_L.

$$F_S \leq F_L$$

IV. METHODS

In order to establish parameters for and test the validity of the model, several experiments were performed with a artificial finger on an experimental eShiver device.

A. eShiver Experimental Apparatus

The experimental apparatus was constructed using a VTS-100 electromagnetic shaker with an anodized aluminum plate mounted parallel to the direction of travel as is shown in Figure 4. The anodized aluminum plate serves as the electroadhesive surface, and its voltage is controlled with a TREK 610C high voltage amplifier while the artificial finger is electrically isolated and grounded. The shaker is driven with a Behringer NU6000 audio amplifier. Displacement is measured with an MTI fiber-optic displacement sensor pointed at the shaker face in the direction of travel. The crossbar holds a linear micrometer slide with fine vertical position adjustment. An ATI Nano17 load cell is mounted to the slide, and the finger mount connects directly to the load cell, holding either the artificial or human finger. All signals were generated and sensors recorded with an NI USB-6361, X Series data acquisition device sampling at $20kHz$.

B. Artificial Finger

Because the mechanical properties of the human skin are highly variable both between subjects and within a single subject over time, a artificial finger was built to approximate the size, shape, bulk stiffness, electrical, and material properties of the human fingertip. The cross-section view of the artificial is shown in Figure 2. The exterior shell is composed of room-temperature-vulcanized silicone rubber (Smooth-On Mold Star 20A) filled with 6% by weight carbon black (Printex XE-2B). The composite rubber material was measured to have a bulk resistivity of roughly 10^3 ohm meters. This shell is adhered to an ABS plastic nut which screws onto a steel mounting rod. The interior cavity is filled with conductive carbon black grease in order to create a conductive path between the steel rod to the shell. A thin circle of latex rubber cut from an anti-static finger cot is adhered to the bottom to form the highly resistive skin of the touch surface. While this paper does not fully justify these design choices, in general the artificial finger is highly resistive electrically, mechanically compliant, and has a smooth and flat contacting surface. It was the result of over 30 prototype fingers. Further information on the design of artificial fingertips can be found in [15].

V. EXPERIMENTS

Four experiments were conducted to measure the electroadhesive friction strength, the lateral mechanical impedance, the electrical impedance, and the net actuation force as various actuation parameters are altered. For each experiment, normal force is set at F_Z = 0.20N before the experiment begins, and is monitored and adjusted between individual trials such that it varies by no more than +/-0.02N.

A. Experiment 1: Friction

For experiment 1, a constant voltage was applied as the surface was slid back and forth beneath the artificial finger at 2 Hz with a total displacement of 7mm. The order of trials was randomized in order to reduce systematic errors such as gradual wear or charge build up, and 3 trials were performed at each voltage level. A single trial consists of 1 second of data, which is then chopped to include only the times where sliding occurs. The mean lateral force while sliding as a function of DC voltage level is shown in Figure 5.

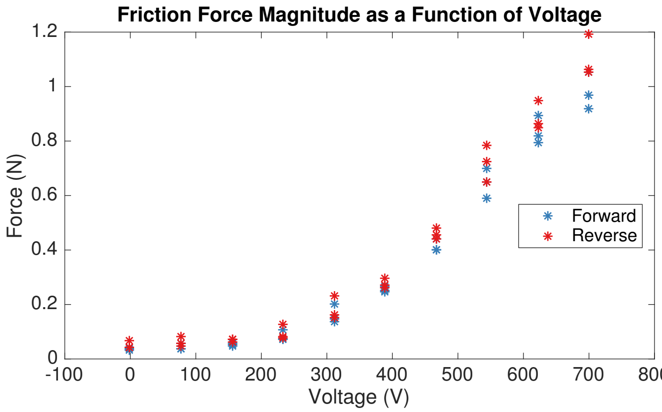

Fig. 5. Mean friction level while sliding as a function of applied voltage.

B. Experiment 2: Mechanical Impedance

For experiment 2, the aluminum plate was replaced with a light-weight carbon fiber plate to which the artificial fingertip was affixed using double-stick tape. The carbon fiber plate was mounted on a brass flexure on one side, and to a Kistler 9203 piezoelectric load cell on the other side. A high resolution MTI edge probe was used to measure displacement at the base of the load cell. The magnitude and phase of the force and velocity data were recorded at each actuation frequency. Each data point represents the mean across 2.5 seconds of data, and 3 trials were performed at each frequency in random order.

This measurement was repeated with the carbon fiber plate only, and the data was found to fit to a pure mass model of 2.4g. Shown in Figure 6, the dynamic model introduced in Figure 2 was fit to the artificial finger data, and the plate mass was subtracted from that model to arrive at the plate mass adjusted impedance of the artificial fingertip. This fit produced parameter values of $m = 0.3g$, $b = 1kg/s$, and $k = 4400N/m$ with a natural frequency near 500Hz. Mean values were reported in [13] for the human finger in the medial-lateral direction of $m = 0.13g$, $b = 1.3kg/s$, and $k = 900N/m$.

C. Experiment 3: Electrical Impedance

In order to measure the values of electrical impedance, a sinusoidal return current of 10uA was commanded, and the resultant voltage at that frequency was measured. Trials are conducted in random order and repeated 3 times at each frequency. Each data point represents the mean across 20 cycles.

This measurement was made for the total impedance, and then repeated in two cases. A measure of the total impedance without the gap impedance was made by applying conductive carbon black grease between the finger and the plate. Finally, a measurement of the artificial finger alone was made by again shorting the gap and replacing the anodized aluminum plate with a conductive plate. Measured impedance across frequency is shown in Figure 7. For ease of interpretation, approximate impedance values at 55Hz relating to the model in Figure 2 are $Z_f = 32 * 10^6 \angle -73\,\text{deg}$, $Z_P = 1 * 10^6 \angle -$

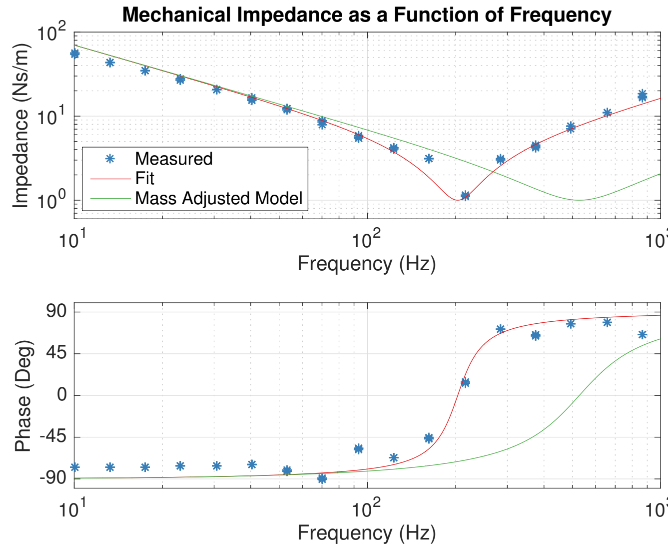

Fig. 6. Measured mechanical impedance of the artificial finger affixed to a carbon fiber plate. Model parameters are fit to the measured data and the model is adjusted to subtract the impedance of the plate.

$35\,\text{deg}$, and $Z_g = 14 * 10^6 \angle -66\,\text{deg}$, where Z_g is taken as $Z_t - Z_f - Z_P$.

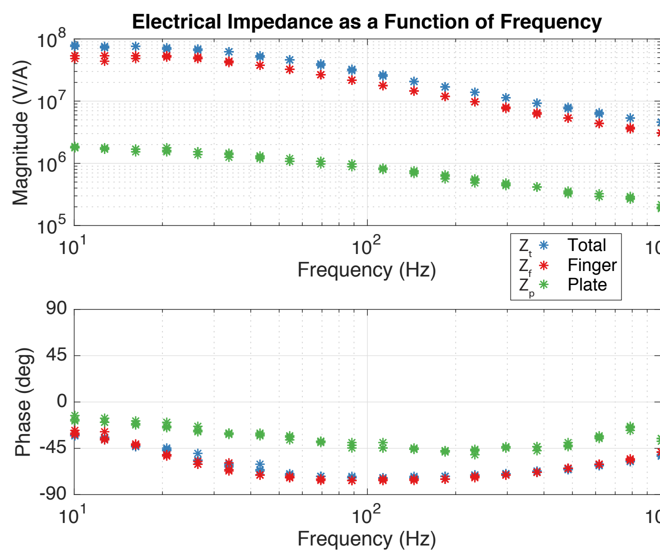

Fig. 7. Electrical impedance measured at 10uA.

The values of these impedance parameters are important for two reasons relevant to the performance of the device. First, impedances in series act as a voltage divider, meaning that the magnitude of the gap voltage, and thus friction force is a function of the relative magnitude of the frequency dependent impedances. Second, there is some phase delay between the actuation voltage and the gap voltage. We note that some parts of this system, in particular the anodized aluminum, behave non-linearly, and impedance results at other currents may not be the same.

D. Experiment 4: Force on the artificial Finger

For experiment 4, the force generated on the artificial finger by the eShiver was measured as actuation parameters were systematically altered. A driving frequency of $55Hz$, a switching frequency of $2Hz$, and a normal force of $0.20N$ were used for the entire experiment. Voltage was commanded as a square wave between zero and the stated voltage. The lateral forces reported for experiment 4 are as measured at the load cell F_Y. Although it is not identically equal to F_S due to the mass, the results of experiment 2 suggest it is equivalent up to frequencies nearing $500Hz$.

Each trial contains a ramp up and ramp down period to smoothly get the shaker up to speed which is discarded in post-analysis. At the switching frequency, the phase of the voltage signal is switched by 180 degrees such that the direction of the force vector reverses. Each trial lasts for one second, the trials are conducted in a random order, and each trial is repeated three times. The directional switches are divided in post-analysis, and the net force, F_{net} is defined as the mean force across a single trial in one switching direction.

1) Experiment 4.1- Varying Phase: For experiment 4.1, the relative phase between the displacement and the applied voltage is varied from zero to 360 degrees. Zero phase for the friction switch is defined as the point where command voltage switches high, such that the phase values in Figure 8 should be interpreted as the phase at which the measured voltage is leading the measured displacement.

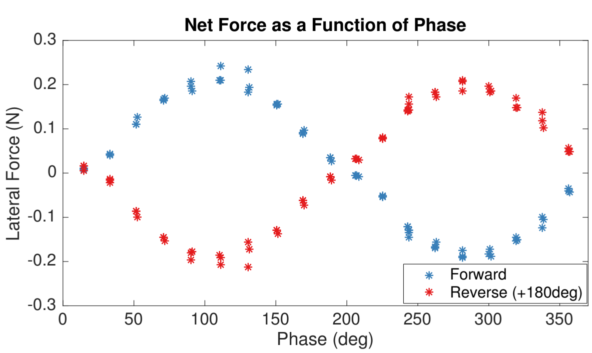

Fig. 8. Lateral force as a function of phase.

Figure 8 shows that the max force is achieved when voltage leads displacement by slightly over 90 degrees. This is interpreted to mean that the optimal time for the friction switch to be on is when the plate is moving in one direction, and that it should be shut off as it reverses direction. Referring back to Figure 6, this is consistent in that the impedance at $55Hz$ is primarily due to the stiffness. As frequency increases, however, it is expected that the optimal switching phase will change to follow the phase of the mechanical impedance.

2) Experiment 4.2- Varying Velocity: For experiment 4.2, a constant voltage is set, phase is set at 275 degrees, and the velocity is varied. For each cycle at $55Hz$, the minimum and maximum forces are found. For each trial, the median values are taken from these minima and maxima and are plotted along with net force in Figure 9. Figure 10 shows the difference between F_{net} in the forward and reverse directions at 225, 550 and $750V$. Comparing Figure 9 to Figure 5, we see that the maximum friction level of roughly $0.6N$ matches the coefficient of friction at $550V$. Interestingly, the minimum friction level is much higher (0.2N) than the coefficient of friction at 0V. This suggests either that the voltage across the gap is not reaching zero, or that the assumption of velocity independent coefficient of friction was invalid.

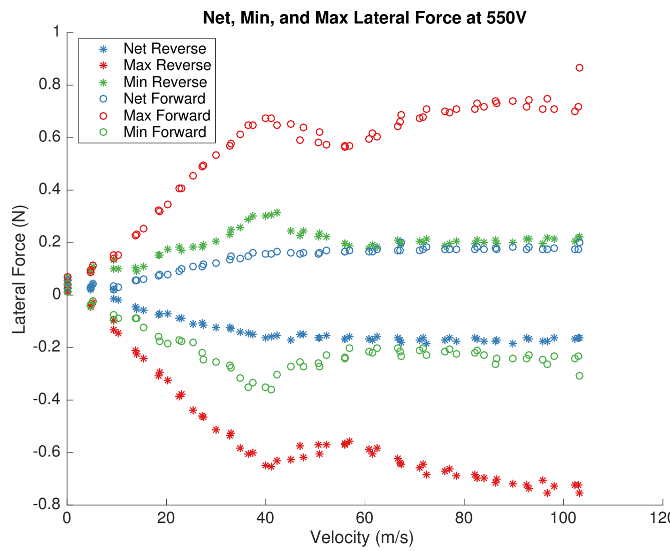

Fig. 9. Minimum, maximum, and net lateral force as a function of velocity.

3) Experiment 4.3- Varying Voltage: For experiment 4.3, constant velocities are set at 15, 29, and $44mm/s$, the phase is set at 275 degrees, and the applied voltage is varied. Figure 11 shows the difference between F_{net} in the forward and reverse directions.

VI. DISCUSSION

Taken together with the proposed model, these plots offer insight into the behavior of the system. There are three ways in which force on the skin F_S may be limited, and these show up as regions in Figures 10 and 11.

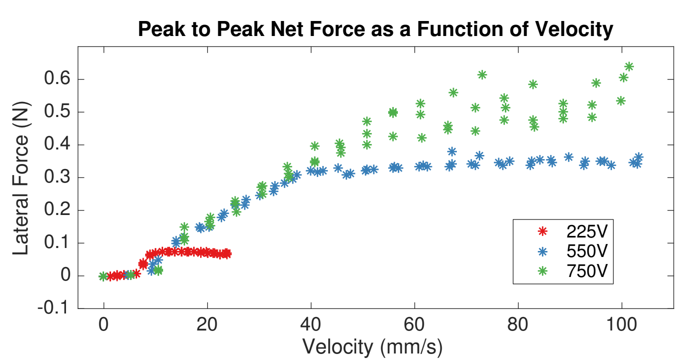

Fig. 10. Lateral force as a function of velocity.

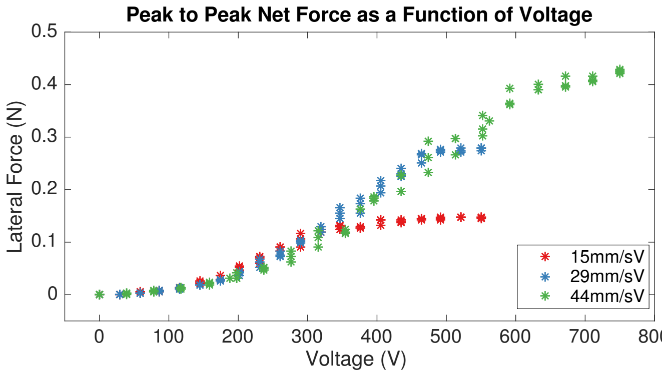

Fig. 11. Lateral force as a function of voltage.

A. Slip Limited

$$F_L < F_{mn}$$

At low velocity the finger is effectively always stuck, resulting in a symmetrical applied force. The interface must slip in the reverse direction in order to create net force, yet it is stuck until the generated force F_L exceeds F_{mn}. This slip limited region is visible in Figure 10 between 0 and $7mm/s$. The net force in this region is zero, and as is shown in Figure 9, the minimum and maximum forces are equal.

B. Lateral Force Limited

$$F_{mn} < F_L < F_{mx}$$

The data in Figure 11 were taken at a constant velocity, such that the finger is not slip limited. At small voltages, F_{mx} barely exceeds F_{mn} and the velocity is such that the finger is sliding in both directions for the majority of the cycle. As voltage is increased, F_{mx} increases, causing an increase in F_{net} that mimics the force proportional to voltage squared increase shown in Figure 5. As voltage increases still further, it surpasses the level needed to keep the finger stuck for the entire high friction portion of the cycle, and F_S is instead limited by the lateral force generated across the impedance F_L. Increasing the velocity increases F_L, and as would be expected, Figure 11 shows that higher velocities asymptote at a higher force.

C. Friction Switch Limited

$$F_{mx} < F_L$$

Referring again to Figure 10 as velocity increases past the slip limit, the data show an increase in net force that is proportional to velocity. As velocity continues to increase however, a limit is reached where increasing velocity further has no effect. At this point, the maximum force of the friction switch is exceeded, and the finger is slipping for the majority of both the forward and reverse portions of the cycle. As would be expected, increasing the voltage level increases this limit.

VII. CONCLUSIONS

A novel haptic display has been developed for applying shear forces to the bare fingertip. The eShiver operates on the same basis as the earlier ShiverPad, but uses electrostatic forces rather than ultrasonic vibrations as a friction switch. A set of experiments performed at the relatively low operating frequency of 55 Hz and using an artificial finger have elucidated the roles of friction, mechanical impedance, and electrical impedance. In ongoing work, these elements are being integrated into a holistic model that will be used to design higher frequency, high force eShiver devices. While an artificial finger cannot fully capture the contact mechanics, lubrication, and multi-scale structure of a real finger, human subject experiments are also underway, and will be reported in a future publication.

ACKNOWLEDGMENT

Special thanks to Craig Shultz and Juan Diego Mena. This material is based upon work supported by the National Science Foundation under Grant No. IIS-1302422.

REFERENCES

[1] A.M. Okamura, “Methods for haptic feedback in teleoperated robotassisted surgery,” Industrial Robot, vol. 31, no. 6, Dec. 2004.

[2] A. Seth, H.-J. Su, and J. M. Vance, “SHARP: a system for haptic assembly and realistic prototyping,” in ASME 2006 International Design Engineering Technical Conferences and Computers and Information in Engineering Conference, 2006, pp. 905912.

[3] E. C. Chubb, J. E. Colgate, and M. A. Peshkin, “ShiverPaD: A Glass Haptic Surface That Produces Shear Force on a Bare Finger,” IEEE Transactions on Haptics, vol. 3, no. 3, pp. 189198, Jul. 2010.

[4] X. Dai, J. E. Colgate, and M. A. Peshkin, “LateralPaD: A surface-haptic device that produces lateral forces on a bare finger,” in 2012 IEEE Haptics Symposium (HAPTICS), 2012, pp. 714.

[5] J. Mullenbach, D. Johnson, J. E. Colgate, and M. A. Peshkin, “ActivePaD surface haptic device,” in 2012 IEEE Haptics Symposium (HAPTICS), 2012, pp. 407414.

[6] G. Robles-De-La-Torre and V. Hayward, “Force can overcome object geometry in the perception of shape through active touch,” Nature, vol. 412, no. 6845, pp. 445448, Jul. 2001.

[7] M. Minsky, “Computational haptics: the sandpaper system for synthesizing texture for a force-feedback display,” Massachusetts Institute of Technology, Cambridge, MA, 1996.

[8] S. Saga and R. Raskar, “Simultaneous geometry and texture display based on lateral force for touchscreen,” in World Haptics Conference (WHC), 2013, 2013, pp. 437442.

[9] D. Wang, K. Tuerz, M. Rossi, and J. Shu, “Haptic overlay device for flat panel touch displays,” in 12th International Symposium on Haptic Interfaces for Virtual Environment and Teleoperator Systems, 2004. HAPTICS 04. Proceedings, 2004, p. 290.

[10] L. Winfield, J. Glassmire, J. E. Colgate, and M. Peshkin, “T-PaD: Tactile Pattern Display through Variable Friction Reduction,” in World Haptics 2007, pp. 421 426.

[11] A. Johnsen, K. Rahbek, “A physical phenomenon and its applications to telegraphy, telephony, etc.,” Electrical Engineers, Journal of the Institution of , vol.61, no.320, pp.713,725, July 1923

[12] C. D. Shultz, M. A. Peshkin, and J. E. Colgate, “Surface haptics via electroadhesion: Expanding electrovibration with Johnsen and Rahbek,” in 2015 IEEE World Haptics Conference (WHC), 2015

[13] M. Wiertlewski and V. Hayward, “Mechanical behavior of the fingertip in the range of frequencies and displacements relevant to touch,” Journal of Biomechanics, vol. 45, no. 11, pp. 18691874, Jul. 2012.

[14] M. Kucharova, S. Doubal, P. Klemera, P. Rejchrt, and M. Navratil, “Viscoelasticity of Biological Materials Measurement and Practical Impact on Biomedicine,” Physiol. Res. 56 (Suppl. 1): S33-S37, 2007

[15] R. F. Friesen, M. Wiertlewski, M. A. Peshkin, and J. E. Colgate, Bioinspired artificial fingertips that exhibit friction reduction when subjected to transverse ultrasonic vibrations, in 2015 IEEE World Haptics Conference (WHC), 2015, pp. 208213.